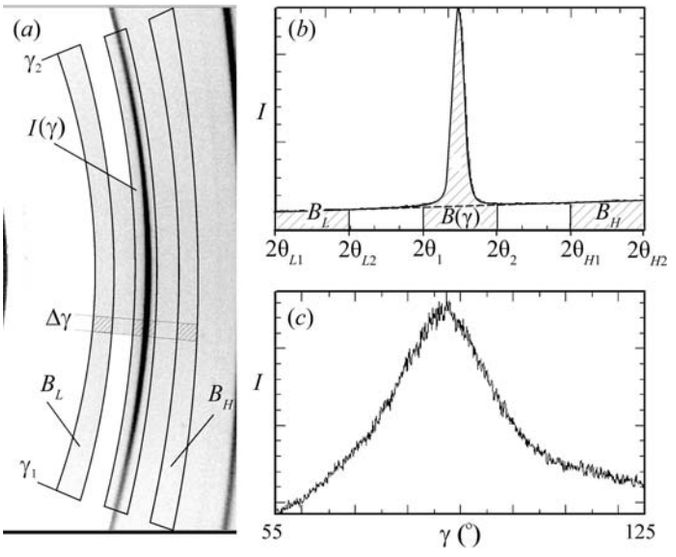

Figure 2.5.21
Pole-figure data processing: (*a*) a frame with the 2θ integration ranges for the (220) ring; (*b*) 2θ profile showing the background and peak; (*c*) integrated intensity distribution as a function of γ.

expressed as

$$I(\gamma) = \int_{2\theta_1}^{2\theta_2} J(2\theta, \gamma)\, \mathrm{d}(2\theta), \quad \gamma_1 \leq \gamma \leq \gamma_2. \tag{2.5.61}$$

A similar equation can be used for 2θ integration of the low and high backgrounds $B_L(\gamma)$ and $B_H(\gamma)$. Assuming a linear background change in the vicinity of the 2θ peak, the background under the peak, $B(\gamma)$, is then given by

$$B(\gamma) = B_L(\gamma)\frac{(2\theta_2 - 2\theta_1)(2\theta_{H2} + 2\theta_{H1} - 2\theta_2 - 2\theta_1)}{(2\theta_{L2} - 2\theta_{L1})(2\theta_{H2} + 2\theta_{H1} - 2\theta_{L2} - 2\theta_{L1})} + B_H(\gamma)\frac{(2\theta_2 - 2\theta_1)(2\theta_2 + 2\theta_1 - 2\theta_{L2} - 2\theta_{L1})}{(2\theta_{H2} - 2\theta_{H1})(2\theta_{H2} + 2\theta_{H1} - 2\theta_{L2} - 2\theta_{L1})}. \tag{2.5.62}$$

Then the background $B(\gamma)$ can be subtracted from the integrated intensity distribution $I(\gamma)$.

The algorithms of γ integration given in Section 2.5.4.2.3 can be easily modified for 2θ integration by exchanging γ and 2θ in the equations. Algorithms with solid-angle normalization should be used to get consistent integrated intensity over all areas of the detector. The 2θ-integrated intensity distribution can then be mapped onto a pole figure based on the fundamental equations (2.5.53) and (2.5.54). When a pole-figure pixel is overlapped by more than one data point from different scans, as shown in the region covered by two scans in Fig. 2.5.20(*b*), the average value should be mapped to that pole-figure pixel. Fig. 2.5.22(*a*) shows pole-density mappings on the pole figure. There are big gaps between the measured pole-density data points due to the large φ-scan steps of 5°.

All factors affecting relative intensities, such as Lorentz, polarization, air scattering, and Be-window and sample absorption, will have an effect on the measured pole densities for the pole figures. Some or all these corrections may be applied to the diffraction frames before 2θ integration if the texture study demands high accuracy in the relative pole densities. Among these factors, the most important factor is sample absorption, since data sets for pole figures are typically collected at several different incident angles. A ridge between the pole-density regions covered by two different incident angles may be observed if sample absorption is not properly corrected.

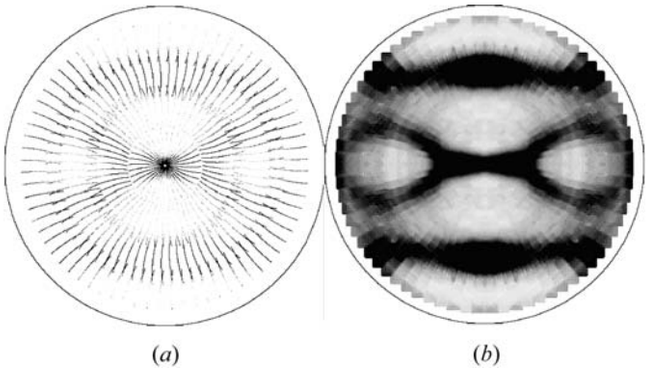

Figure 2.5.22
Pole-figure processing: (*a*) $I(\gamma)$ mapped to the pole figure; (*b*) Pole figure after interpolation and symmetry processing.

2.5.4.2.5. *Pole-figure interpolation and use of symmetry*

The pole figure is stored and displayed as a bitmap image. The pole-density data from the data set may not fill up all the pixels of the pole-figure image. In order to generate a smooth pole figure, the unmapped pixels are filled with values generated from the interpolation of the surrounding pixels. A linear interpolation within a defined box is sufficient to fill the unmapped pixels. The size of the box should be properly chosen. A box that is too small may not be able to fill all unmapped pixels and a box that is too big may have a smearing effect on the pole figure, especially if a sharp pole figure is processed. All the gaps between the measured pole-density points are filled after this interpolation. For a sample with sharp texture, smaller φ-scan steps should be used.

All pole figures possess symmetry as a consequence of the Laue symmetry of the crystallites in the sample. This symmetry can be used to fill in values for pixels in the pole figure for which data were not measured, or to smooth the pole figure. For example, orthorhombic materials exhibit *mmm* symmetry, thus one needs to collect only an octant or quadrant of the pole sphere to generate the entire pole figure. The pole figures of materials with higher symmetry may be treated by using lower symmetry in the processing. For instance, one can use 2/*m* or *mmm* symmetry for hexagonal materials and *mmm* for cubic materials. In symmetry processing, all the symmetry-equivalent pole-figure pixels are filled by the average value of the measured pixels. For the unmeasured pole-figure pixels, this symmetry processing fills in a value from the average of all the equivalent pixels. For the measured pixels, this average processing serves as a smoothing function. Fig. 2.5.22(*b*) shows the results after both interpolation and use of symmetry.

2.5.4.2.6. *Orientation relationship*

A 2D-XRD system can measure texture from a sample containing a single phase, multiple phases or single crystals. The orientation relationship between different phases, or thin films and substrates, can be revealed because data are collected from all phases of the sample simultaneously. One example is the measurement of pole figures for a magnetron sputter-deposited Cu film on an Si wafer (He *et al.*, 2005). Fig. 2.5.23 shows the overlapped pole figures of the Cu (111) film and Si (400) substrate in a 2D pole figure (*a*) and 3D surface plot (*b*). The three sharp spots from the (400) spots of the Si wafer show the wafer cut orientation of (111). The Cu (111) pole density maxi-

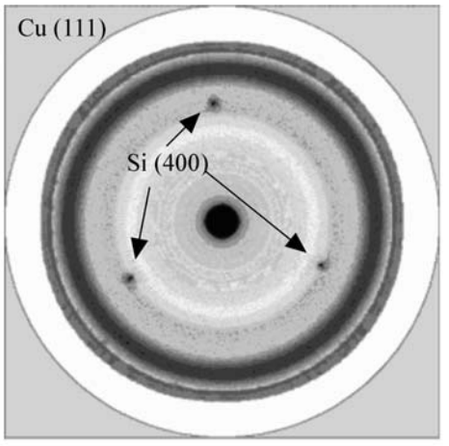

(*a*)

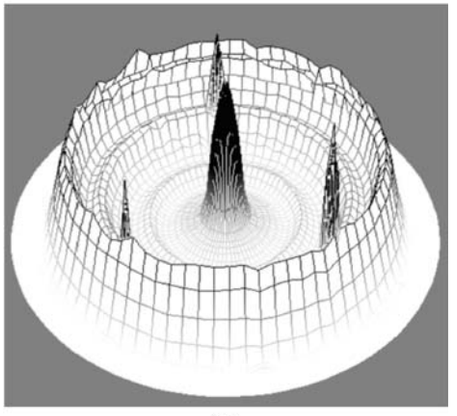

(*b*)

Figure 2.5.23
Combined pole figure of a Cu (111) film on an Si (400) substrate: (*a*) regular 2D projection; (*b*) 3D surface plot.

mized in the centre of the pole figure shows a strong (111) fibre texture. The orientation relationship between the film fibre axis and the substrate is clearly described by the combined pole figures. For samples containing multiple thin-film layers, the orientation relationships between the different layers of the films and substrate can be revealed by superimposing their pole figures.

2.5.4.3. *Stress measurement*

When a solid material is elastically deformed by a force, each crystallite in it changes shape or size. Assuming that the stresses in each crystallite represent the stresses in the solid, the stresses can be measured by measuring the lattice *d*-spacing changes in the crystallites. These *d*-spacing changes can be measured by the changes in diffraction-peak positions based on Bragg's law. In this case, the *d*-spacing serves as a gauge of the deformation. Stress measurement by X-ray diffraction is typically done using a point detector or line detector (Walter, 1971; James & Cohen, 1980; Noyan & Cohen, 1987; Lu, 1996); this will be referred to as the conventional method. The stress or stress tensor is calculated from many strain measurements from diffraction-peak 2θ shifts of a specific lattice-plane family. With a point or line detector, only a small cross section of the diffraction cone is measured at one sample orientation (ψ, φ). Compared to using a conventional detector, 2D detectors have many advantages in stress measurement (Borgonovi, 1984; Korhonen *et al.*, 1989; Yoshioka & Ohya, 1992; Fujii & Kozaki, 1993; He & Smith, 1997; Kämpfe *et al.*, 1999; Hanan *et al.*, 2004). Since a 2D diffraction pattern covers the whole or a large portion of the diffraction rings, it can be used to measure stress with higher accuracy and can be collected in a shorter time than a conventional diffraction pattern, especially when dealing with highly textured materials, large grain sizes, small sample areas, weak diffraction, stress mapping and stress-tensor measurement. The 2D method for stress measurement is based on the fundamental relationship between the stress tensor and the diffraction-cone distortion (He & Smith, 1997; He, 2000; European Standard, 2008).

There are two kinds of stresses, which depend on the source of the loading forces that produce them. One kind is applied stress, caused by external forces acting on the solid object. Applied stress changes when the loading forces change and it disappears once the forces are removed. The stresses measured by X-ray diffraction method are mostly residual stresses. Residual stress is caused by internal forces between different parts of a solid body. Residual stress exists without external forces or remains after the external forces have been removed. The net force and moment on a solid body in equilibrium must be zero, so the residual stresses in the body must be balanced within the body. This means that a compressive stress in one part of the body must come with a tensile stress in another part of the body. For example, the residual stress in a thin film is balanced by the stresses in the substrate. When residual stress in a solid body is mentioned it typically refers to a specific location.

Residual stresses are generally categorized as macroscopic or microscopic depending on the range over which the stresses are balanced. The macroscopic residual stress is the stress measured over a large number of grains. This kind of stress can be measured by X-ray diffraction through the shift of the Bragg peaks. The microscopic stress is the stress measured over one or a few grains, or as small a range as micro- or nanometres. This kind of stress alone will not cause a detectable shift of diffraction peaks, but is reflected in the peak profiles. In this chapter, we will focus on the X-ray diffraction method for stress measurement at the macroscopic level.

2.5.4.3.1. *Stress and strain relation*

Stress is a measure of the deforming force applied to a solid per unit area. The stress on an elemental volume in the sample coordinates S_1, S_2, S_3 contains nine components, given by

$$\sigma_{ij} = \begin{bmatrix} \sigma_{11} & \sigma_{12} & \sigma_{13} \\ \sigma_{21} & \sigma_{22} & \sigma_{23} \\ \sigma_{31} & \sigma_{32} & \sigma_{33} \end{bmatrix}. \tag{2.5.63}$$

A component is normal stress when the two indices are identical, or shear stress when the two indices differ. The group of the nine stress components is called the stress tensor. The stress tensor is a tensor of the second order. Under equilibrium conditions, the shear components must maintain the following relations:

$$\sigma_{12} = \sigma_{21},\ \ \sigma_{23} = \sigma_{32} \text{ and } \sigma_{31} = \sigma_{13}. \tag{2.5.64}$$

Therefore, only six independent components define the stress state in a solid. The following stress states are typically measured:

Uniaxial: all stress components are zero except one normal stress component.

Biaxial: all nonzero components are within the S_1S_2 plane.

Biaxial with shear: $\sigma_{33} = 0$, all other components are not necessarily zero.

Equibiaxial: a special case of biaxial stress where $\sigma_{11} = \sigma_{22} = \sigma$.